

Gravity waves excited by jets: Propagation versus generation

R. Plougonven

School of Mathematics and Statistics, University of St. Andrews, St. Andrews, UK

C. Snyder

National Center for Atmospheric Research, Boulder, Colorado, USA

Received 6 June 2005; revised 10 August 2005; accepted 18 August 2005; published 17 September 2005.

[1] Atmospheric jets are known to be an important source of inertia-gravity waves, yet remain poorly understood as such. Previous studies on the subject have concentrated on the generation mechanisms for the gravity waves, with the underlying assumption that the characteristics of the waves were imposed by the generation mechanism. In proceeding so, effects due to the propagation of the waves through a complex three-dimensional flow have been overlooked. Using numerical simulations of idealized baroclinic instability in a periodic channel, we show that propagation effects can determine several characteristics of the gravity waves emitted into the middle atmosphere from tropospheric jets. Specifically, the numerical simulations demonstrate that the propagation of inertia-gravity waves through horizontal deformation and vertical shear strongly influences the spatial organization of the waves and imposes the 3D orientation of their wave-vector. **Citation:** Plougonven, R., and C. Snyder (2005), Gravity waves excited by jets: Propagation versus generation, *Geophys. Res. Lett.*, 32, L18802, doi:10.1029/2005GL023730.

1. Introduction

[2] As general circulation models are extended to higher altitudes, it is necessary to better understand the tropospheric sources of gravity waves which provide a crucial forcing to the circulation of the Middle Atmosphere [Fritts and Alexander, 2003]. In particular, tropospheric jets are known to be significant sources of gravity waves, yet the reasons for this remain poorly understood. Another motivation for the investigation of gravity waves excited by jets is the turbulence that they can induce in the lower stratosphere, above the jet stream [Lane et al., 2004].

[3] Intense inertia-gravity waves associated to jets are often observed in the vicinity of the jet-exit regions, either near a ridge [Uccellini and Koch, 1987; Guest et al., 2000], or near a trough [Plougonven et al., 2003]. Numerical studies investigating gravity wave excitation in idealized baroclinic life-cycles have also found that gravity waves typically appear in jet-exit regions [O'Sullivan and Dunkerton, 1995; Zhang, 2004]. Both sorts of studies have generally argued in consequence that the gravity waves are generated in the jet-exit region.

[4] To date, such arguments have ignored how propagation through the time-dependent, three-dimensional baroclinic flow might influence the observed and simulated gravity waves. The importance of propagation effects is,

however, clear in simpler problems. Geostrophic adjustment within a flow as simple as a barotropic zonal jet already differs significantly from the standard scenario because the jet modifies the propagation of the gravity waves [Plougonven and Zeitlin, 2005]. Studies of gravity-wave generation in two-dimensional frontogenesis [Snyder et al., 1993; Reeder and Griffiths, 1996] have also illustrated that the propagation of the excited waves can explain essential features of the wave pattern.

[5] In this article, we analyse gravity waves spontaneously generated in simulations of an idealized baroclinic life cycle and show that the propagation of the waves sets several of their characteristics. In the lower stratosphere, the gravity waves concentrate in specific regions of the flow with strong horizontal deformation and vertical shear. We show that simple considerations of linear propagation may explain the location of the waves and provide predictions for the 3D orientation of their wave-vector [Bühler and McIntyre, 2005].

2. Propagation in a Deformation Flow With Vertical Shears

[6] We present here an effect recently highlighted by Bühler and McIntyre [2005] (previously identified by Badulin and Shrira [1993]), which these authors have called 'wave capture.' Consider as a steady background flow the superposition of a horizontal deformation field and vertical shears:

$$\mathbf{U} = (U, V) = (-\alpha x + \beta z, \alpha y + \gamma z). \quad (1)$$

[7] We obtain the evolution of the three components of the wavenumber $\mathbf{k} = (k, l, m)$ of a gravity wave packet from the ray-tracing equations [Lighthill, 1978]:

$$D_g(k, l, m) = \left(-\frac{\partial \Omega}{\partial x}, -\frac{\partial \Omega}{\partial y}, -\frac{\partial \Omega}{\partial z} \right). \quad (2)$$

where $D_g = \partial/\partial t + \mathbf{c}_g \cdot \nabla$ is the total derivative along a ray, $\Omega = \tilde{\omega} + \mathbf{k} \cdot \mathbf{U}$ is the absolute frequency of the wave packet, and $\tilde{\omega}$ is the intrinsic frequency.

[8] Using (1) in (2), and integrating from (k_0, l_0, m_0) as the initial wavevector, we obtain:

$$(k, l, m) = \left(k_0 e^{\alpha t}, l_0 e^{-\alpha t}, m_0 - \frac{\beta}{\alpha} k_0 (e^{\alpha t} - 1) + \frac{\gamma}{\alpha} l_0 (e^{-\alpha t} - 1) \right). \quad (3)$$

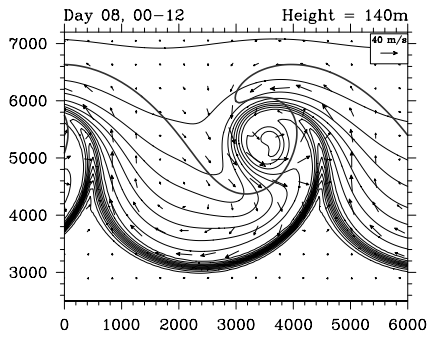


Figure 1. Mature stage of the baroclinic life-cycle, depicted by the potential temperature near the surface ($z = 140$ m, contours every 1.25 K) at day 08, 12:00. Also shown as a thick line is the 3 pvu line at $z = 8$ km, to suggest the deformation of the tropopause aloft. The domain is 4000 km long and periodic in x ; for clarity, one and a half periods are shown.

[9] Provided the wave vector is not initially purely along the y axis, it tends to infinity at an exponential rate given by the deformation α , and aligns with the direction given by

$$(\alpha^2 + \beta^2)^{-1/2}(\alpha, 0, \beta). \quad (4)$$

[10] As the wavelengths of the waves shrink, the group velocity of the wavepacket vanishes and it is advected toward the dilatation axis taken from the stagnation point (the y -axis in the above) and concentrates there [Bühler and McIntyre, 2005].

[11] The above theoretical arguments ignore the possibility of additional spatial or temporal variations of the background flow. Nevertheless, from these simple theoretical considerations we may form three predictions to test in simulations of baroclinic life cycles:

[12] 1. Regions within the baroclinic wave where the horizontal deformation is large and where the flow relative to the baroclinic wave is weak will play a key role in organizing the gravity wave field.

[13] 2. The wavevector of the gravity waves will align with a direction, given by (4), that one can obtain from a coarse-grained knowledge of the background flow.

[14] 3. The wavelengths of the gravity waves will decrease and their phase lines in the horizontal will align with the local dilatation axis as they approach the region of wave capture.

3. Model Setup and Baroclinic Life Cycle

[15] The Weather Research and Forecast Model [Skamarock et al., 2005] is used to simulate the evolution of baroclinic instability of a jet on the f -plane, in a channel that is periodic in the x direction. The domain is 4000 km in x , 10000 km in y , and 20 km deep. The upper boundary is a free surface. Below we will concentrate on moderate-resolution simulations having 50 km grid spacing in the horizontal and 250 m in the vertical. A Smagorinski scheme with fourth-order diffusion provides dissipation.

[16] The initial state consists of a superposition of a purely zonal jet in geostrophic equilibrium and its most unstable normal mode with a small amplitude. The zonal jet is obtained in a fashion similar to Rotunno et al. [1994]. A sharp tropopause separates the troposphere (with uniform potential vorticity (PV) of 0.4 PVU) from the stratosphere (with uniform PV of 4 PVU).

[17] During the first 7 to 8 days, the normal mode grows exponentially, as expected. The evolution of the mature baroclinic instability then becomes nonlinear (Figure 1): strong fronts form near the surface and a tongue of warm air rolls up cyclonically. Once the instability has saturated, a strong cyclonic vortex dominates the flow from the surface to the lower stratosphere.

[18] Gravity waves are seen clearly in several locations by day 7 (not shown), in particular above and below the jet.

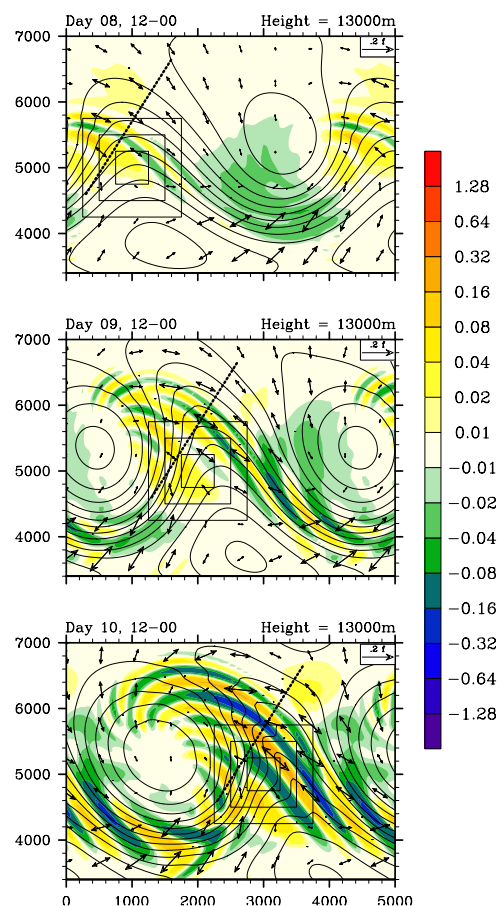


Figure 2. Maps of divergence of the horizontal wind at $z = 13$ km, for day 8, 12:00 (upper panel), day 9, 12:00 (middle panel) and day 10, 12:00. Contours of the divergence are logarithmic, as shown by the label bar (units are 10^{-4}s^{-1}). Double arrows indicate the direction and intensity of the local deformation. Potential temperature is indicated by the black lines (contour every 5K). The squares indicate the volumes over which averages of the background deformation and vertical shears were calculated. The thick dashed line shows the location of the cross-sections shown in Figure 3. In the last panel, note a secondary wavepacket, near $x = 2000$ km and $y = 3800$ km, that is also oriented along the local dilatation axis.

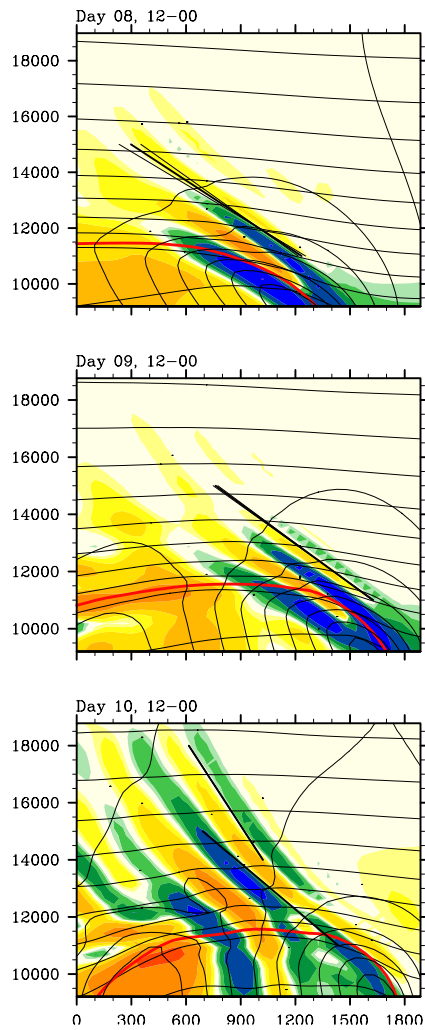


Figure 3. Vertical cross-sections along the dotted lines indicated in Figure 2. Vertical axis shows altitude in m, the horizontal axis shows distance in km along the cross-section. The background flow is depicted by normal velocity and potential temperature as black contours (every 10 ms^{-1} and 10 K respectively), and the tropopause (3 pvu) as the thick red line. Colors indicate the divergence of horizontal wind, with the same contours as in Figure 2. The black line segments show the slope obtained according to (4), from averages of the background flow taken in the squares shown in Figure 2 and at most between 11 and 15 km. To show the spread of the slopes obtained from averaging over different volumes, three lines are plotted, corresponding to the mean, and \pm one standard deviation. Except in the upper panel, the three lines are indistinguishable. Finally, in the lower panel, the slope obtained from averaging over volumes between 14 and 18 km is also shown.

We will focus on the gravity waves that propagate into the lower stratosphere above the jet.

4. Results

[19] The divergence of horizontal wind is used to identify the gravity waves present in the flow [Plougouven

and Teitelbaum, 2003]. Horizontal cross-sections of the wave field in the lower stratosphere are displayed in Figure 2. In agreement with the arguments of section 2, we find that regions with strong horizontal deformation play a key role in organizing the gravity-wave field, and that the phase lines tend to align with the dilatation axis.

[20] To compare the orientation of the wave vector with the prediction (4), the mean deformation ($\alpha = 0.5 \sqrt{(\partial u/\partial x - \partial v/\partial y)^2 + (\partial u/\partial y + \partial v/\partial x)^2}$) and vertical shear ($\gamma = \partial u_{\text{contr}}/\partial z$, where u_{contr} is the component of velocity parallel to the contraction axis), of the flow were obtained by averaging over large volumes of fluid. (As shown in Figure 3, the predicted orientation varies little as the dimensions of the volume over which the averages are calculated varies from 500 to 1500 km in the horizontal, and from 1 to 4 km in the vertical.)

[21] The vertical cross-sections of Figure 3 show a striking agreement between the slope of the phase lines and that predicted by (4). Furthermore, as expected from section 2, the wavelengths decrease as the wave packet approaches the dilatation axis.

[22] Finally, the amplitude of the gravity waves is very sensitive to the resolution, but their location and orientation is not (Figure 4). The dependence of the wavelength on model resolution is consistent with the theoretical arguments of section 2 and the finite resolution and dissipation of the model. In the simulations, a balance between the small-scale dissipation and the tendency for the wavelength to decrease (cf. (3)) is attained. Since the dissipation is decreased as the resolution increases,

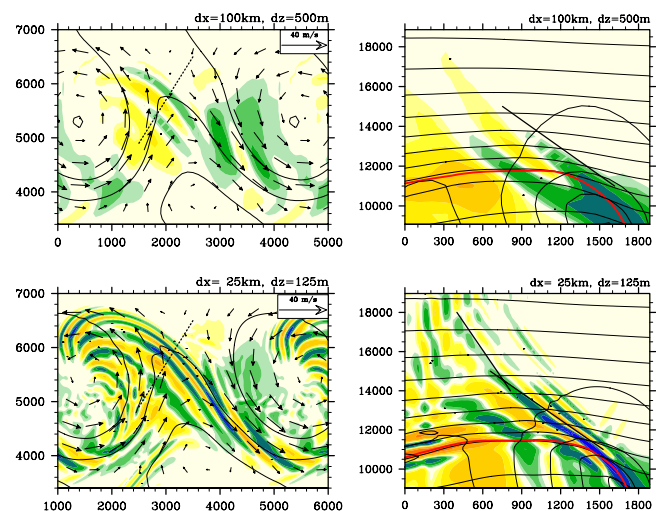


Figure 4. Horizontal and vertical cross-sections of the horizontal divergence at lower ($dx = 100 \text{ km}$, $dz = 500 \text{ m}$, upper panel) and higher ($dx = 25 \text{ km}$, $dz = 125 \text{ m}$ lower panel) resolution, to be compared with the middle panels of Figures 2 and 3. (Contrary to Figure 2, the arrows here show the wind relative to the (propagating) baroclinic wave, in order to highlight the stagnation point and the dilatation axis.) In agreement with section 2, the wavelengths decrease as resolution increases. Moreover, the high-resolution simulation clearly shows the wavelengths decreasing spatially as the waves approach the dilatation axis.

the minimum wavelength of the simulated waves also decreases.

5. Discussion

[23] We have investigated one mechanism that contributes to determine several characteristics of inertia-gravity waves spontaneously excited in simulations of idealized baroclinic waves. Simple theoretical arguments describing the linear propagation of a gravity wave packet in a background flow made of a superposition of horizontal deformation flow and vertical shears [Bühler and McIntyre, 2005] led to the formulation of three predictions in section 2: 1) that regions with strong horizontal deformation, especially those near stagnation points in the flow relative to the baroclinic wave, would play a key role in organizing the gravity-wave field (Figure 2), 2) that the wave vectors would align with a direction obtained from coarse-grained knowledge of the background flow (Figure 3), and 3) that the wavelengths of the waves would tend to decrease as they approached this stagnation point.

[24] Good (Figure 2) to excellent (Figures 3 and 4) agreement with these predictions was found. Furthermore, these predictions were verified regardless of the resolution of the simulations, possibly explaining why low-resolution operational analyses contain gravity waves whose characteristics (location, orientation, intrinsic frequency) are in qualitative agreement with observations [Plougonven and Teitelbaum, 2003].

[25] The information obtained here on the gravity waves comes only from considering their propagation. Hence we intend this example to suggest that propagation effects have been somewhat overlooked, and that they may provide valuable keys to understand the gravity waves that are generated from jets and fronts.

[26] This example has important implications. First, if this mechanism is a significant factor determining the location and characteristics of the gravity waves, it becomes more difficult to infer how and where the waves were emitted. Second, this mechanism decreases the scale of the waves, possibly leading to their breaking [Bühler and McIntyre, 2005], which will be of importance for turbulence and mixing [Lane *et al.*, 2004].

[27] Finally, although the case presented above is suggestive, it is only one case. Further research is underway to determine how general this mechanism is, and to address the question of the amplitude of the excited waves.

[28] **Acknowledgments.** The authors thank D.J. Muraki for fruitful interactions on this problem. R.P. is grateful to O. Bühler and M. McIntyre

for stimulating discussions, Bill Skamarock and Wei Wang for valuable help with the simulations. R.P. acknowledges support from the French government (Bourse *'Initiative Post-doc'*), and from the Nuffield Foundation (Award to Newly Appointed Lecturers). C.S. was partially supported by NSF grant 0327582. NCAR's Scientific Computing Division provided the resources for the high-resolution simulations.

References

- Badulin, S. I., and V. I. Shrira (1993), On the irreversibility of internal waves dynamics due to wave-trapping by mean flow inhomogeneities. Part 1. Local analysis, *J. Fluid Mech.*, *251*, 21–53.
- Bühler, O., and M. E. McIntyre (2005), Wave capture and wave-vortex duality, *J. Fluid Mech.*, *534*, 67–95.
- Fritts, D. C., and M. J. Alexander (2003), Gravity wave dynamics and effects in the middle atmosphere, *Rev. Geophys.*, *41*(1), 1003, doi:10.1029/2001RG000106.
- Guest, F., M. Reeder, C. Marks, and D. Karoly (2000), Inertia-gravity waves observed in the lower stratosphere over Macquarie Island, *J. Atmos. Sci.*, *57*, 737–752.
- Lane, T. P., J. D. Doyle, R. Plougonven, R. D. Sharman, and M. A. Shapiro (2004), Numerical modeling of gravity waves and shearing instabilities above an observed jet, *J. Atmos. Sci.*, *61*, 2692–2706.
- Lighthill, J. M. (1978), *Waves in Fluids*, Cambridge Univ. Press, New York.
- O'Sullivan, D., and T. J. Dunkerton (1995), Generation of inertia-gravity waves in a simulated life cycle of baroclinic instability, *J. Atmos. Sci.*, *52*(21), 3695–3716.
- Plougonven, R., and H. Teitelbaum (2003), Comparison of a large-scale inertia-gravity wave as seen in the ECMWF and from radiosondes, *Geophys. Res. Lett.*, *30*(18), 1954, doi:10.1029/2003GL017716.
- Plougonven, R., and V. Zeitlin (2005), Lagrangian approach to the geostrophic adjustment of frontal anomalies in a stratified fluid, *Geophys. Astron. Fluid Dyn.*, *99*(2), 101–135.
- Plougonven, R., H. Teitelbaum, and V. Zeitlin (2003), Inertia-gravity wave generation by the tropospheric mid-latitude jet as given by the FASTEX radiosoundings, *J. Geophys. Res.*, *108*(D21), 4686, doi:10.1029/2003JD003535.
- Reeder, M. J., and M. Griffiths (1996), Stratospheric inertia-gravity waves generated in a numerical model of frontogenesis. Part II: Wave sources, generation mechanisms and momentum fluxes, *Q. J. R. Meteorol. Soc.*, *122*, 1175–1195.
- Rotunno, R., C. Snyder, and W. C. Skamarock (1994), An analysis of frontogenesis in numerical simulations of baroclinic waves, *J. Atmos. Sci.*, *51*(23), 3373–3398.
- Skamarock, W. C., J. B. Klemp, J. Dudhia, D. O. Gill, D. M. Barker, W. Wang, and J. G. Powers (2005), A description of the Advanced Research WRF, version 2, *NCAR Tech. Note, 468+STR*, Natl. Cent. for Atmos. Res., Boulder, Colo.
- Snyder, C., W. C. Skamarock, and R. Rotunno (1993), Frontal dynamics near and following frontal collapse, *J. Atmos. Sci.*, *50*(18), 3194–3211.
- Uccellini, L. W., and S. E. Koch (1987), The synoptic setting and possible energy sources for mesoscale wave disturbances, *Mon. Weather Rev.*, *115*, 721–729.
- Zhang, F. (2004), Generation of mesoscale gravity waves in upper-tropospheric jet-front systems, *J. Atmos. Sci.*, *61*(4), 440–457.

R. Plougonven, School of Mathematics and Statistics, University of St. Andrews, North Haugh, St. Andrews, KY16 9SS, UK. (riwal.plougonven@polytechnique.org)

C. Snyder, National Center for Atmospheric Research, Boulder, CO 80307-3000, USA.